Aust. J. Phys., 1986, **39**, 871–80

Particle–Hole Description of Dipole States in ^{17}O

J. A. Eden and Y. I. Assafiri

School of Physics, University of Melbourne,
Parkville, Vic. 3052.

Abstract

The particle–hole model has been applied to the ^{17}O nucleus to study the electric dipole states below the giant dipole resonance (GDR). Comparison is made with the most recent photonuclear data for this nucleus and an E1 assignment for the observed strength at 15·1 MeV in the photoproton cross section is discussed. The WMBH residual interaction used in this calculation produces more $T_>$ strength below the GDR than predicted in other calculations using the Tabakin, Soper or Kuo–Brown interactions.

1. Introduction

The photoproton cross section for ^{17}O has been measured from threshold to 43 MeV by Zubanov *et al.* (1984) and shows a prominent resonance near 15·1 MeV. Such a feature is not observed in the photoneutron cross section by Jury *et al.* (1980) for this nucleus at the same energy. If we assume that this structure can be described by one-particle (1p) or two-particle one-hole (2p–1h) wavefunctions, its isospin must be either $T = \frac{1}{2}$ ($T_<$) or $T = \frac{3}{2}$ ($T_>$) (see Fig. 1). The $T_<$ possibility is immediately rejected since neutron emission from these states is known to be strong in this energy region due to the many $T = 0$ energetically accessible states in the daughter nucleus. The lowest $T = 1$ state in ^{16}O occurs at 12·8 MeV. Consequently, decay via neutron emission from $T_>$ states below 16·9 MeV in ^{17}O is suppressed by isospin selection rules. This identifies the 15·1 MeV structure as $T_>$.

The spin and parity assignments for this observed structure have been open to debate. An electron scattering experiment by Rangacharyulu *et al.* (1983) found excitations at 15·1 MeV to be predominantly M1 with some E2 contribution. Attempts were made to fit with E1, M1, E2 and M2 excitations, but good agreement could only be obtained with M1 and E2. The M1 excitations from the ground state of $^{17}O(J^\pi = \frac{5}{2}^+)$ can populate only $(\frac{3}{2}, \frac{5}{2}, \frac{7}{2})^+$ states. Since the strength is known to be $T_>$, isobaric analogue states should exist in ^{17}N and ^{17}F. Rangacharyulu *et al.* identified the state at 4·000 MeV in $^{17}N(J^\pi = \frac{3}{2}^{(-)})$ as the likely isobaric analogue to the 15·1 MeV resonance observed, suggesting its tentative parity assignment is incorrect. The corresponding isobaric analogue in ^{17}F has not yet been found.

The photoneutron angular distribution for ^{17}O leading to the ground state in ^{16}O has been measured by Jury *et al.* (1985), who suggested that E1 transitions make up

0004-9506/86/060871$02.00

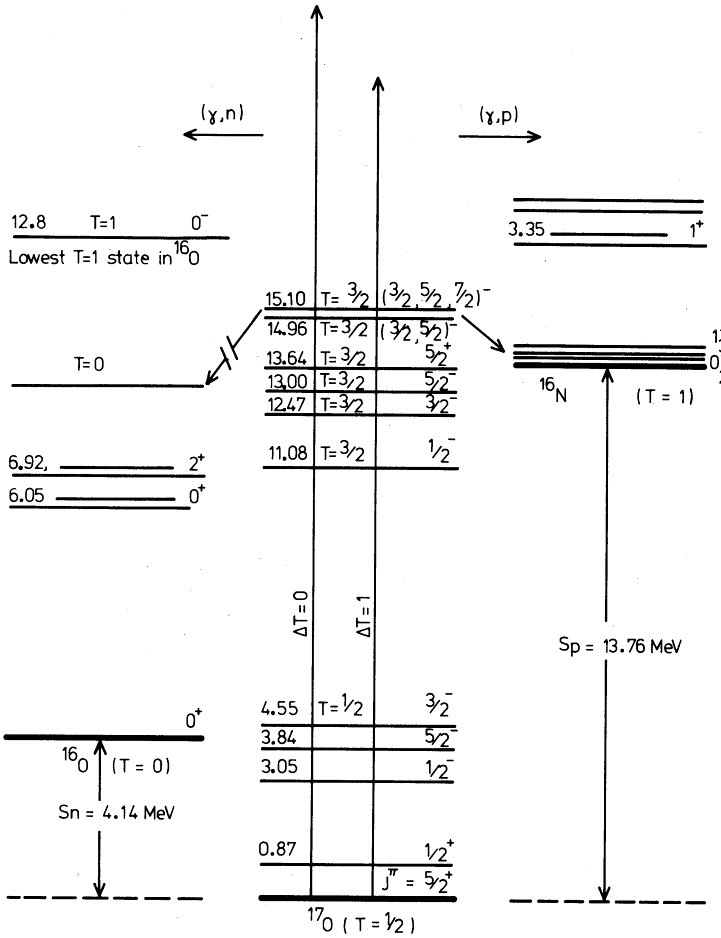

Fig. 1. Energy level diagram for single nucleon emission from excited states in ^{17}O. The E1 selection rules are $\Delta l = 0, \pm 1$ and $\Delta T = 0, +1$.

nearly all the absorption strength in the region studied (10–24 MeV), except in narrow regions near 11, 12, 15·1, 15·9, 17·3 and 22·3 MeV. In these regions the a_1 Legendre coefficient is small but notably nonzero. With consideration of the significant M1 and E2 absorption seen by Snover *et al.* (1983) in experiments on ^{16}O, the nonzero values were interpreted by Jury *et al.* as evidence of M1 or E2 strength interfering with the (assumed) dominant E1 strength of the pygmy resonance.

The results of both these experiments suggest that M1 absorption strength exists near 15·1 MeV in ^{17}O. For this reason it has been suggested that the strength seen in the ^{17}O photoproton cross section at 15·1 MeV results from M1 photo-absorption. However, this strength cannot be accounted for by the assumption of pure M1 photo-excitation. The Gell-Mann–Telegdi (1953) sum rule, given by

$$\int \sigma_0(\mathrm{M1}, \omega)\, \frac{\mathrm{d}\omega}{\omega} = \frac{\pi^2}{137}\left(\frac{\hbar}{Mc}\right)^2 \frac{1}{4\hbar^2}\langle [L + \{2(\mu_\mathrm{p} + \mu_\mathrm{n})/\mu_0\} S]^2 \rangle_{\mathrm{g.s.}}, \tag{1}$$

leads to a value of 0·048 mb if a $1d_{5/2}$ single-particle ground state wavefunction is assumed. However, the preliminary data of Zubanov *et al.* (1984) indicate that the inverse energy weighted sum rule, when evaluated over the 15·1 MeV resonance in the ^{17}O photoproton cross section, gives a value of $0 \cdot 1 \pm 0 \cdot 02$ mb. We note that the photoproton cross section near 15·1 MeV accounts for only a fraction of the total photo-absorption in the same energy region. In addition, M1 absorption is believed to occur at other energies in ^{17}O. The inverse energy weighted cross section over the 15·1 MeV resonance in the photoproton cross section exceeds the entire M1 inverse energy weighted photo-absorption cross section. Thus, the structure near 15·1 MeV is unlikely to result purely from M1 photo-absorption.

It is proposed that the structure near 15·1 MeV in the ^{17}O photoproton cross section is due predominately to E1 photo-absorption. This implies the existence of a state or states of spin and parity $J^{\pi} = (\frac{3}{2}, \frac{5}{2}, \frac{7}{2})^{-}$. This suggestion does not preclude the existence of positive parity states near 15·1 MeV.

Population of $T_{>}$ states via electric dipole photo-absorption can be fairly well predicted by the p–h model with a suitable choice of nucleon–nucleon interaction. Such a calculation is presented here to support the proposed E1 absorption near 15·1 MeV in the ^{17}O photoproton cross section. The Wigner–Majorana–Bartlett–Heisenberg (WMBH) interaction is selected in view of its success in many similar applications (e.g. Gillet and Vinh Mau 1964; Cooper and Eisenberg 1968; Fraser *et al.* 1970; Assafiri and Morrison 1984). In other calculations which predict the dipole strengths of states in mass 17 nuclei, a variety of interactions have been used. Albert *et al.* (1977) used a Tabakin interaction, which predicts no $T_{>}$ strength below the GDR, and a Soper interaction, which predicts weak fragmented strength below the GDR. The Soper interaction required an increased weighting for the $J^{\pi} = 2^{+}$ intermediate coupling for $T_{<}$ states to obtain agreement with the available data. Harekeh *et al.* (1975) have used a Kuo–Brown interaction and predicted very weak $T_{>}$ strength at energies as low as 15 MeV.

2. Formalism

Basis Configurations

In the p–h model, the average nucleon field is given by

$$H_0 = \sum_{\alpha} \epsilon_{\alpha}\, a_{\alpha}^{\dagger}\, a_{\alpha}\,, \tag{2}$$

where the ϵ_{α} are the unperturbed single-particle energies chosen from experimental data and α labels the spherical single-particle basis. The full Hamiltonian is written in the second quantisation formalism as

$$H = \sum_{\alpha\beta} a_{\alpha}^{\dagger}(\alpha\,|\,t\,|\,\beta)a_{\beta} + \tfrac{1}{2} \sum_{\alpha\beta\delta\gamma} a_{\alpha}^{\dagger}\, a_{\beta}^{\dagger}(\alpha\beta\,|\,v\,|\,\delta\gamma)a_{\gamma}\, a_{\delta}\,, \tag{3}$$

where

$$(\alpha\beta\,|\,v\,|\,\delta\gamma) = \int \mathrm{d}(1)\,\mathrm{d}(2)\; \Phi_{\alpha}^{*}(1)\; \Phi_{\beta}^{*}(2)\; v(1,2)\; \Phi_{\delta}(1)\; \Phi_{\gamma}(2)\,, \tag{4}$$

and $\Phi_{\alpha}(i)$ are the single-particle wavefunctions, chosen to be those of a harmonic oscillator.

The *jj* coupling scheme is chosen to describe the system and its basis configurations. Valence neutron excitations to the p–f shell have been ignored. Any odd parity states whose wavefunctions include significant p–f shell single-particle configurations will have an unacceptably large energy uncertainty due to the gross discrepancies in p–f shell single-particle energies quoted elsewhere [see Harekeh *et al.* (1975) for a more detailed discussion]. All odd parity states are constructed from 2p–1h configurations in the p and s–d shells. This truncation of basis configurations has no effect on $T_>$ states.

The 2p–1h configurations are specified by

$$|(1)(2)J_0\, T_0(\mathrm{h})^{-1}J\,T\rangle = N^{-1}\sum_m (j_1\, m_{j_1}\, j_2\, m_{j_2}\,|\, J_0\, M_{J_0})(J_0\, M_{J_0}\, j_\mathrm{h} - m_{j_\mathrm{h}}\,|\, J M_J)$$
$$\times(\tfrac{1}{2} m_{\tau_1}\, \tfrac{1}{2} m_{\tau_2}\,|\, T_0\, M_{T_0})(T_0\, M_{T_0}\, \tau_\mathrm{h} - m_{\tau_\mathrm{h}}\,|\, T M_T)a_\mathrm{h}\, a_2^\dagger\, a_1^\dagger\,|\mathrm{core}\rangle, \tag{5}$$

where

$$N^2 = 1-\phi(1 j_1\, j_2\, J_0\, T_0)\delta_{12}, \tag{6}$$
$$a_i \equiv a_{(nljm_jm_\tau)_i}, \qquad (i)\equiv(nlj)_i,$$

with

$$\delta_{\alpha\beta} = \delta_{n_\alpha n_\beta}\,\delta_{l_\alpha l_\beta}\,\delta_{j_\alpha j_\beta}, \qquad \phi(abc\ldots)\equiv(-1)^{a+b+c\ldots}.$$

The set of shell-model configurations that span a particular (J, T) subspace is obtained by listing all configurations of the required (J, T) and then rejecting null configurations using equation (6).

Residual Interaction

The notation used here is the same as that by Cooper and Eisenberg (1968). The residual nucleon–nucleon interaction used is the standard central force given by

$$v(1,2) = f(|r_1-r_2|)(a_{00}+a_{10}\,\boldsymbol{\sigma}_1\cdot\boldsymbol{\sigma}_2+a_{01}\,\boldsymbol{\tau}_1\cdot\boldsymbol{\tau}_2+a_{11}\,\boldsymbol{\sigma}_1\cdot\boldsymbol{\sigma}_2\,\boldsymbol{\tau}_1\cdot\boldsymbol{\tau}_2), \tag{7}$$

with the strength normalised by

$$a_{00}+a_{10}-3a_{01}-3a_{11} = 1, \tag{8}$$
$$f(|r_1-r_2|) = -V_0\exp[-\{(r_1-r_2)/r_0\}^2]. \tag{9}$$

The matrix elements of (7) taken between 2p states coupled to good angular momentum and isospin (J and T) has been given by Cooper and Eisenberg (1968).

Matrix Elements of the Hamiltonian

Matrix elements between 1p configurations are given by

$$\langle(1')|H|(1)\rangle = E_0+\epsilon_1\,\delta_{11'}; \tag{10}$$

those between 1p and 2p–1h configurations by

$$\langle(1')|H|(1)(2)J_0\, T_0(\mathrm{h})^{-1}J\,T\rangle = \frac{1}{N}\,\phi(j_\mathrm{h}\,\tfrac{1}{2}J_0\, T_0\, J\,T)\frac{\hat{J}_0\,\hat{T}_0}{\hat{J}\hat{T}}\,\delta_{Jj_1}\,\delta_{T\frac{1}{2}}\,\tilde{V}_{J_0T_0}(1'\mathrm{h};12); \tag{11}$$

and those between 2p–1h configurations by

$$\langle(1')(2')J_0'\, T_0'(\mathrm{h}')^{-1}J\,T|H|(1)(2)J_0\, T_0(\mathrm{h})^{-1}J\,T\rangle = V_0+V_\mathrm{pp}+V_\mathrm{ph}; \tag{12}$$

where

$$V_0 = (E_0+\epsilon_1+\epsilon_2-\epsilon_h)\delta_{hh'}\delta_{11'}\delta_{22'}\delta_{J_0J_0'}\delta_{T_0T_0'},$$

$$V_{pp} = \frac{1}{NN'}\tilde{V}_{J_0T_0}(1'2';12)\,\delta_{hh'}\delta_{J_0J_0'}\delta_{T_0T_0'},$$

$$V_{ph} = \frac{\delta_{22'}}{NN'}\hat{J}_0\hat{J}_0'\hat{T}_0\hat{T}_0'\phi(1j_1j_h J_0J_0'T_0T_0')$$

$$\times\sum_{LM}\begin{bmatrix} j_h' & J & J_0' \\ j_1 & J_0 & j_2 \\ L & j_h & j_1'\end{bmatrix}\begin{bmatrix} \frac{1}{2} & T & T_0' \\ \frac{1}{2} & T_0 & \frac{1}{2} \\ M & \frac{1}{2} & \frac{1}{2}\end{bmatrix}\tilde{V}_{LM}(1'h;h'1)\,\phi(LM)(\hat{L}\hat{M})^2$$

$$+\frac{\delta_{11'}}{NN'}\hat{J}_0\hat{J}_0'\hat{T}_0\hat{T}_0'\phi(1j_2'j_h)$$

$$\times\sum_{LM}\begin{bmatrix} j_h' & J & J_0' \\ j_2 & J_0 & j_1 \\ L & j_h & j_2'\end{bmatrix}\begin{bmatrix} \frac{1}{2} & T & T_0' \\ \frac{1}{2} & T_0 & \frac{1}{2} \\ M & \frac{1}{2} & \frac{1}{2}\end{bmatrix}\tilde{V}_{LM}(2'h;h'2)\,\phi(LM)(\hat{L}\hat{M})^2$$

$$-\frac{\delta_{12'}}{NN'}\hat{J}_0\hat{J}_0'\hat{T}_0\hat{T}_0'\phi(1j_1j_h J_0'T_0')$$

$$\times\sum_{LM}\begin{bmatrix} j_h' & J & J_0' \\ j_2 & J_0 & j_1 \\ L & j_h & j_1'\end{bmatrix}\begin{bmatrix} \frac{1}{2} & T & T_0' \\ \frac{1}{2} & T_0 & \frac{1}{2} \\ M & \frac{1}{2} & \frac{1}{2}\end{bmatrix}\tilde{V}_{LM}(1'h;h'2)\,\phi(LM)(\hat{L}\hat{M})^2$$

$$-\frac{\delta_{1'2}}{NN'}\hat{J}_0\hat{J}_0'\hat{T}_0\hat{T}_0'\phi(j_1j_2j_2'j_h J_0T_0)$$

$$\times\sum_{LM}\begin{bmatrix} j_h' & J & J_0' \\ j_1 & J_0 & j_2 \\ L & j_h & j_2'\end{bmatrix}\begin{bmatrix} \frac{1}{2} & T & T_0' \\ \frac{1}{2} & T_0 & \frac{1}{2} \\ M & \frac{1}{2} & \frac{1}{2}\end{bmatrix}\tilde{V}_{LM}(2'h;h'1)\,\phi(LM)(\hat{L}\hat{M})^2,$$

and where

$$\tilde{V}_{JT}(12;34) = V_{JT}(12;34)-\phi(1j_3j_4JT)\,V_{JT}(12;43), \tag{13}$$

$$\hat{J}\equiv(2J+1)^{\frac{1}{2}}.$$

The E_0 and ϵ_j used above are given by

$$E_0 = \sum_{\lambda\epsilon\text{core}}\left|(\lambda|t|\lambda)+\tfrac{1}{2}\sum_{\omega\epsilon\text{core}}\{(\lambda\omega|v|\lambda\omega)-(\lambda\omega|v|\omega\lambda)\}\right|, \tag{14}$$

which enters the shell-model calculation as an overall constant to obtain a convenient zero energy and

$$\epsilon_i \delta_{ij} = (i|t|j) + \sum_{\lambda \in \mathrm{core}} \{(i\lambda|v|j\lambda) - (i\lambda|v|\lambda j)\}, \tag{15}$$

which are the single-particle energies chosen from experiment (Jolly 1963). Spurious states are removed using the second method described by Assafiri and Morrison (1984).

Dipole Photo-excitation

The integrated cross section $\sigma_{\mathrm{I}}(\mathrm{f}\leftarrow\mathrm{i})$ describing the excitation of the final nuclear state $|\mathrm{f}\rangle$ from the initial nuclear state $|\mathrm{i}\rangle$ through absorption of a photon of energy $\hbar\omega_{\mathrm{fi}}$ and polarisation $\hat{\epsilon}$ is given in the dipole approximation by (Cooper and Eisenberg 1968)

$$\begin{aligned}\sigma_{\mathrm{I}}(\mathrm{f}\leftarrow\mathrm{i}) &= \int \sigma_{\mathrm{fi}}(\omega)\, \mathrm{d}(\hbar\omega) \\ &= \frac{4\pi^2 e^2}{\hbar c} \hbar\omega_{\mathrm{fi}} \left|\langle \mathrm{f}| \sum_{\alpha\beta} a_\alpha^\dagger (\alpha| \boldsymbol{r}.\hat{\epsilon}\tfrac{1}{2}(1+\tau_z)|\beta) a_\beta |\mathrm{i}\rangle\right|^2 .\end{aligned} \tag{16}$$

Using $\lambda_k^\dagger = (m\omega/2\hbar)^{\frac{1}{2}} x_k - (2m\hbar\omega)^{-\frac{1}{2}} P_k$ $(k = 1, 2, 3)$, we find

$$\boldsymbol{r}.\hat{\epsilon} = (2a^2)^{-\frac{1}{2}}\{\lambda_\nu^\dagger + (-1)^\nu \lambda_{-\nu}\}, \tag{17}$$

where $a = (m\omega/\hbar)^{\frac{1}{2}}$ is the oscillator range parameter.

The second term in the braces of equation (17) refers to photon emission and is not relevant to this dipole photo-absorption calculation. After averaging over polarisation and angular momentum quantum numbers and identifying $\hbar\omega_{\mathrm{fi}} = E_{\mathrm{f}} - E_{\mathrm{i}}$, we find

$$\begin{aligned}\sigma_{\mathrm{I}}(\mathrm{f}\leftarrow\mathrm{i}) &= \frac{\pi^2 e^2}{2a^2} \frac{\hbar\omega_{\mathrm{fi}}}{\hbar c} \tfrac{1}{3}(\hat{J}'/\hat{J})^2 \left|\sum_{\alpha\beta} \langle \mathrm{f}| a_\alpha^\dagger a_\beta |\mathrm{i}\rangle\langle\alpha|\lambda_\nu^\dagger(1+\tau_z)|\beta\rangle\right|^2 \\ &= \frac{15}{51}(\hat{J}')^2 \Bigg| \sum_{\mathrm{if}} \frac{X_{\mathrm{i}}\, Y_{\mathrm{f}}\, \hat{J}_0'\, \hat{T}_0'}{N'} \begin{Bmatrix} \frac{1}{2} & \frac{1}{2} & T_0' \\ \frac{1}{2} & T' & 1 \end{Bmatrix} \phi(T'\tfrac{1}{2}) \\ &\quad \times \left(\langle 2' \| \lambda^\dagger \| \mathrm{h}' \rangle \begin{Bmatrix} j_1 & j_2' & J_0' \\ j_{\mathrm{h}}' & J' & 1 \end{Bmatrix} \phi(j_1\, j_2'\, j_{\mathrm{h}}'\, J')\delta_{11'} \right. \\ &\quad \left. + \langle 1' \| \lambda^\dagger \| \mathrm{h}' \rangle \begin{Bmatrix} j_1 & j_1' & J_0 \\ j_{\mathrm{h}}' & J' & 1 \end{Bmatrix} \phi(j_{\mathrm{h}}'\, J_0'\, T_0'\, J')\delta_{12'} \right) \Bigg|^2 ,\end{aligned} \tag{18}$$

where

$$\begin{aligned}\langle \alpha \| \lambda_\nu^\dagger \| \beta \rangle &= \phi(1\, l_\alpha\, \tfrac{1}{2} j_\beta) \hat{j}_\alpha \hat{j}_\beta \begin{Bmatrix} j_\beta & 1 & j_\alpha \\ l_\alpha & \frac{1}{2} & l_\beta \end{Bmatrix} [(2 l_\beta\, n_\beta)^{\frac{1}{2}} \delta_{l_\beta, l_\alpha+1}\, \delta_{n_\alpha, n_\beta+1} \\ &\quad + \{(l_\beta+1)(2n_\beta + 2l_\beta + 1)\}^{\frac{1}{2}} \delta_{l_\alpha, l_\beta+1}\, \delta_{n_\alpha, n_\beta}],\end{aligned} \tag{19}$$

and X_{i} and Y_{f} are the eigenvector components of the shell-model configurations. Obviously for a single-particle ground state $X_{\mathrm{i}} \equiv 1$, i.e. a single configuration is used to describe the ground state wavefunction.

Table 1. Parameters for the WMBH interaction

$\epsilon_{1p_{3/2}}$ (MeV)	$\epsilon_{1p_{1/2}}$ (MeV)	$\epsilon_{1d_{5/2}}$ (MeV)	$\epsilon_{2s_{1/2}}$ (MeV)	$\epsilon_{1d_{3/2}}$ (MeV)	V_0 (MeV)	r_0 (fm)	ar_0	a_{00}	a_{10}	a_{01}	$\hbar\omega$ (MeV)
0	6·15	17·67	18·54	22·75	60·0	1·56	1·0	0·0125	−0·1375	−0·2875	17·0

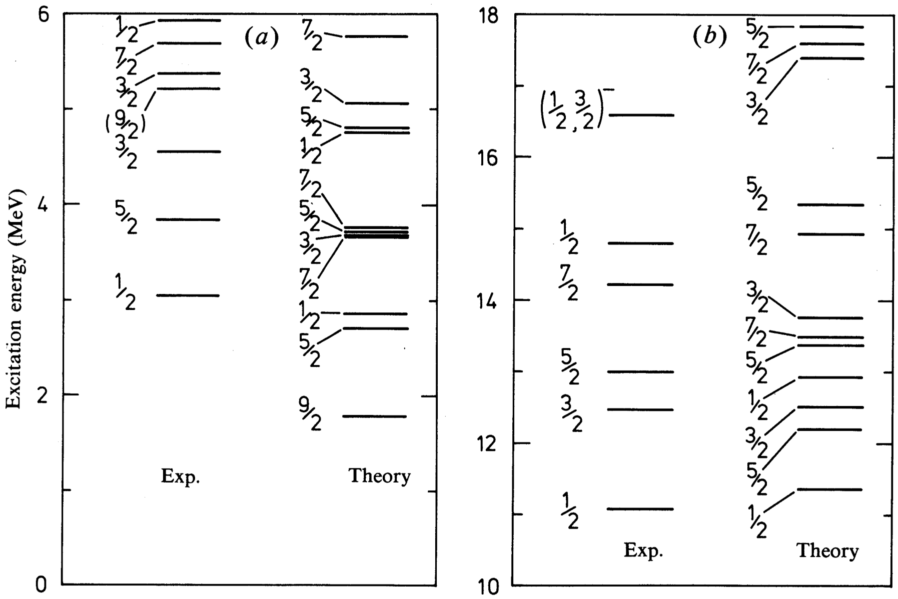

Fig. 2. Energy level diagrams for the experimental and calculated low-lying odd parity states: (a) $T_<$ states and (b) $T_>$ states.

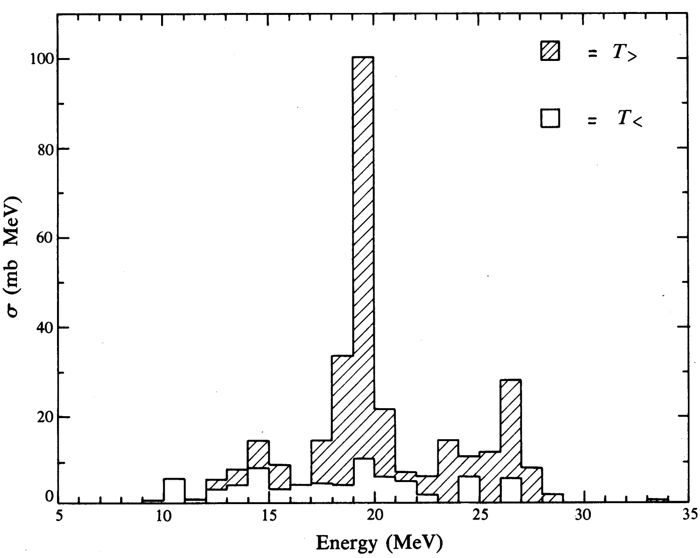

Fig. 3. Calculated electric dipole absorption for ^{17}O showing the relative $T_<$ and $T_>$ strengths. The splitting of the isospin strength can be clearly seen.

3. Results and Discussion

The parameters and single-particle energies used in the present calculation are taken from Assafiri and Morrison (1984) for the case of ^{18}O and are listed in Table 1. Shown in Fig. 2 are the energy levels for the calculated and experimentally determined (Ajzenberg-Selove 1982) low-lying odd parity states in ^{17}O (doubtful states are shown in parentheses). Some resemblance to the experimental data is observed. A detailed study of the ground state has been made by Brown and Green (1966), indicating that the $1d_{5/2}$ single-particle ground state wavefunction used in this calculation describes 81% of the complete ground state wavefunction. Whilst simple interactions such as WMBH cannot be expected to accurately describe all experimentally observed states, it is expected that some of the discrepancies observed in Fig. 2 result from the use of a simplistic single-particle ground state wavefunction. The importance of higher order configurations is evident by the large number of low-lying even parity states that exist below the GDR. In general, an adequate description of these wavefunctions requires the inclusion of 3p–2h, and possibly higher order, configurations. (Even parity states are not included in this calculation.)

Fig. 3 shows the electric dipole photo-absorption strengths for population of $T_<$ and $T_>$ states, plotted in running bins of 1 MeV. The centroid energies for the $T_<$ and $T_>$ photo-absorption strengths are located at 17·8 MeV and 20·9 MeV respectively. Their separation compares favourably with the value 5·3 MeV predicted by Fallieros and Goulard (1970) for this nucleus. The ratio of the inverse energy weighted cross section for $T_>$ and $T_<$ components is given by (Diener *et al.* 1971)

$$\int \sigma_> E^{-1}\,\mathrm{d}E \Big/ \int \sigma_< E^{-1}\,\mathrm{d}E = \frac{1}{T_0}\left|\frac{1-1\cdot 5\,T_0/A^{2/3}}{1+1\cdot 5/A^{2/3}-4\,T_0(T_0+1)/A^2}\right|. \tag{20}$$

For ^{17}O this ratio is predicted to be 1·5, which compares favourably with the value 2·0 obtained for the present calculation. The integrated photo-absorption strengths for population of $T_<$ and $T_>$ states are 89 and 234 mb MeV respectively, summing to 1·27 times the value from the TRK sum rule ($60NZ/A$ mb MeV).

Of particular interest to this study is the experimentally observed structure at 15·1 MeV in the ^{17}O photoproton cross section. This structure accounts for about 6% of the photoproton cross section between 0 and 40 MeV. To evaluate the fraction of the total photo-absorption cross section exhausted by this structure, the total photo-absorption strength is approximated by the sum of the photoneutron and photoproton cross sections. Since the ^{17}O photoneutron cross section shows no obvious structure near 15·1 MeV, the fraction of the total photo-absorption cross section exhausted by the structure of interest can be approximated by (with energies in MeV)

$$\int_{14\cdot 4}^{16\cdot 0} \sigma(\gamma,\mathrm{p})\,\mathrm{d}E \Big/ \int_0^{40} \sigma(\gamma,\mathrm{p})+\sigma(\gamma,s\mathrm{n})\,\mathrm{d}E\,. \tag{21}$$

where $\sigma(\gamma,\mathrm{p})$ represents the cross section for the reaction ^{17}O(γ,p) and $\sigma(\gamma,s\mathrm{n})$ the summed cross sections for all reactions leading to photoneutron emission.

The preliminary data of Zubanov *et al.* (1984) and Jury *et al.* (1980) indicate that the fraction of the total photo-absorption cross section exhausted by the structure of interest, in the approximation (21), is about 1%. However, there is reason to believe this approximation underestimates the true value of this fraction. The structure of interest lies only 1·3 MeV above the reaction threshold and exhibits a distinct asymmetry. This suggests that the Coulomb barrier markedly supresses proton emission in favour of other decay channels.

The present calculation predicts states at 14·9 MeV (J^{π}; $T = \frac{7}{2}^-; \frac{3}{2}$) and 15·3 MeV ($J^{\pi}$; $T = \frac{5}{2}^-; \frac{3}{2}$) exhausting 1·9% and 1·7% of the total dipole photo-absorption cross section respectively. This $T_>$ structure may be associated with that observed experimentally at 15·1 MeV. The wavefunctions for these states show very little configuration admixing, suggesting that the observed strength is largely the result of single-particle excitations of $1p_{1/2}$ nucleons into the $2s_{1/2}$ subshell. It is interesting to note that the stronger $T_>$ states listed in Table 2 are relatively pure. Indeed, if a state with an admixture of many configurations is to exhibit significant dipole strength, coherence between these configurations is required to avoid destructive interference. This coherence is not generally guaranteed.

Table 2. Wavefunctions with their dominant configurations for low-lying $T_>$ dipole states

Energy (MeV)	$J^{\pi}; T$	σ (mb)	Wavefunction
12·2	$\frac{5}{2}^-; \frac{3}{2}$	0·947	$0\cdot718\lvert(1d_{5/2})^1(2s_{1/2})^1[2](1p_{1/2})^{-1}\rangle - 0\cdot638\lvert(1d_{5/2})^2[2](1p_{1/2})^{-1}\rangle$
12·5	$\frac{3}{2}^-; \frac{3}{2}$	1·255	$0\cdot697\lvert(1d_{5/2})^1(2s_{1/2})^1[2](1p_{1/2})^{-1}\rangle - 0\cdot619\lvert(1d_{5/2})^2[2](1p_{1/2})^{-1}\rangle$
13·4	$\frac{5}{2}^-; \frac{3}{2}$	1·277	$0\cdot731\lvert(1d_{5/2})^2[2](1p_{1/2})^{-1}\rangle + 0\cdot621\lvert(1d_{5/2})^1(2s_{1/2})^1[2](1p_{1/2})^{-1}\rangle$
13·5	$\frac{7}{2}^-; \frac{3}{2}$	0·866	$0\cdot896\lvert(1d_{5/2})^2[4](1p_{1/2})^{-1}\rangle + 0\cdot357\lvert(1d_{5/2})^1(2s_{1/2})^1[2](1p_{3/2})^{-1}\rangle$
13·8	$\frac{3}{2}^-; \frac{3}{2}$	1·439	$0\cdot692\lvert(1d_{5/2})^2[2](1p_{1/2})^{-1}\rangle - 0\cdot595\lvert(1d_{5/2})^1(2s_{1/2})^1[2](1p_{1/2})^{-1}\rangle$
14·9	$\frac{7}{2}^-; \frac{3}{2}$	6·074	$0\cdot990\lvert(1d_{5/2})^1(2s_{1/2})^1[3](1p_{1/2})^{-1}\rangle$
15·3	$\frac{5}{2}^-; \frac{3}{2}$	5·430	$0\cdot958\lvert(1d_{5/2})^1(2s_{1/2})^1[3](1p_{1/2})^{-1}\rangle + 0\cdot220\lvert(1d_{5/2})^2[2](1p_{3/2})^{-1}\rangle$

Below the photoproton emission threshold in ^{17}O, $T_>$ states can neutron decay only if they have $T_<$ admixtures. These states are expected to be relatively long-lived, and should appear as sharp structure in the photoneutron cross section. This calculation predicts such $T_>$ strength between 12·2 and 13·5 MeV, and it is suggested this may correspond to the sharp peaks seen in the pygmy resonance of the photoneutron cross section measured by Jury *et al.* (1980).

Table 2 gives the dominant p–h configurations of the low-lying $T_>$ wavefunctions described above. The p–p intermediate-spin couplings are given in square brackets.

Previous calculations to predict the isospin splitting of the GDR using different interactions (e.g. the Soper exchange interaction used by Albert *et al.* 1977) have also found weak $T_>$ dipole states below the main strength of the GDR. One of the distinct differences in the results presented in this study is in the increased strength of these $T_>$ dipole states. The increased fragmentation of the $T_>$ components of the GDR probably arises from the inclusion of isospin and space-exchange contributions to the nucleon–nucleon interaction.

4. Conclusions

The particle–hole model has been applied to the ^{17}O nucleus using a WMBH nucleon–nucleon interaction. The results show significant $T_>$ dipole strength below the main strength of the GDR. In particular, the strength of the $T_>$ dipole states at 14·9 MeV ($J^{\pi}; T = \frac{7}{2}^{-}; \frac{3}{2}$) and 15·3 MeV ($J^{\pi}; T = \frac{5}{2}^{-}; \frac{3}{2}$) suggests that E1 absorption describes most of the observed strength at 15·1 MeV in the ^{17}O photoproton cross section.

Acknowledgments

We wish to thank D. Zubanov and the Livermore group for providing access to the ^{17}O photoproton data prior to publication. We also extend thanks to M. N. Thompson for many helpful discussions.

References

Ajzenberg-Selove, F. (1982). *Nucl. Phys.* A **375**, 1.
Albert, D., Nagl, A., George, I., Wagner, R. F., and Überall, H. (1977). *Phys. Rev.* C **16**, 503.
Assafiri, Y. I., and Morrison, I. (1984). *Nucl. Phys.* A **427**, 460.
Brown, G. E., and Green, A. M. (1966). *Nucl. Phys.* **75**, 401.
Cooper, B. S., and Eisenberg, J. M. (1968). *Nucl. Phys.* A **114**, 184.
Diener, E. M., Amann, J. F., Paul, P., and Blatt, S. L. (1971). *Phys. Rev.* C **3**, 2303.
Fallieros, S., and Goulard, B. (1970). *Nucl. Phys.* A **147**, 593.
Fraser, R. F., Garnsworthy, R. K., and Spicer, B. M. (1970). *Nucl. Phys.* A **156**, 489.
Gell-Mann, M., and Telegdi, V. L. (1953). *Phys. Rev.* **91**, 169.
Gillet, V., and Vinh Mau, N. (1964). *Nucl. Phys.* **54**, 321.
Harekeh, M. N., Paul, P., and Gorodetzky, Ph. (1975). *Phys. Rev.* C **11**, 1008.
Jolly, H. P. (1963). *Phys. Lett.* **5**, 289.
Jury, J. W., Berman, B. L., Faul, D. D., Meyer, P., and Woodworth, J. G. (1980). *Phys. Rev.* C **21**, 503.
Jury, J. W., Watson, J. D., Rowley, D., Phillips, T. W., and Woodworth, J. G. (1985). *Phys. Rev.* C **32**, 1817.
Rangacharyulu, C., Ansalda, E. J., Bender, D., Richter, A., and Spamer, E. (1983). *Nucl. Phys.* A **406**, 493.
Snover, K. A., Adelberger, P. G., Ikossi, P. G., and Brown, B. A. (1983). *Phys. Rev.* C **27**, 1837.
Zubanov, D., Thompson, M. N., Berman, B. L., Pywell, R. E., Jury, J. W., and McNeill, K. G. (1984). Proc. Tenth AINSE Conf. on Nuclear Physics, Paper 63 (AINSE: Canberra).

Manuscript received 8 May, accepted 10 June 1986